NOBLE USE OF SHAPE MEMORY ALLOY IN SEISMIC RETROFIT OF MULTI-SPAN SIMPLY SUPPORTED ELEVATED HIGHWAY

A. K. M. T. A. Khan*& M. A. R. Bhuiyan

Department of Civil Engineering, Chittagong University of Engineering and Technology, Chittagong, Bangladesh
**Corresponding Author: thohidul.ce@gmail.com*

ABSTRACT
Laminated rubber bearings (LRB) are one of the widely used isolation devices in elevated highway for mitigation of seismic induced damages. This isolation bearing has some consequences problems due to strong motions which may causes detrimental effects such as instability of the bearing, pounding, unseating problems of the deck and permanent deformation of the bearings. Shape memory alloy (SMA) bars are known for their super-elastic properties, which have been utilized in various applications in the fields of engineering and science. More recently, these materials have been evaluated for applications in the domain of earthquake engineering. SMAs are unique materials with a substantial potential for retrofitting of elevated highway when incorporated with LRB. The novelty of SMAs lies in their ability to undergo large deformations and return to their undeformed shape through stress removal or shape memory effect. SMAs also have some surprising thermo-mechanical properties, including super-elasticity and hysteretic damping. All these features make this materials a promising solution for blending with LRB to minimize possible seismic risk of bridges which further justified by nonlinear dynamic analysis. This study investigates the effectiveness of SMA based rubber bearing (SRB) in compare to lead rubber bearing to reduce the seismic vulnerability of an elevated highway when subjected to far-field (FF) ground excitations that are spectrally matched to a target design spectrum. The seismic response quantities in the analysis include the absolute maximum values of pier displacement, bearing displacement, deck displacement, deck acceleration, bearing force and residual displacement. The numerical result shows that, the SMA bars are effective in limiting the seismic responses, particularly the residual displacement when blended with LRB. The combined strengths obtained from LRB and SMA bars offers an optimum synergy for bridge retrofitting. Both the Ni-Ti and Cu-Be-Al SMA alloy based rubber bearing proves their superiority in compare to the lead rubber bearing and the evidences focused by the analytical scheme.

Keywords: Shape memory alloy bar; laminated rubber bearing; nonlinear dynamic analysis; super-elasticity behaviour; seismic performance; retrofitting; elevated highway

INTRODUCTION
Laminated rubber bearings are one of widely used devices in seismic isolation of bridges and buildings. They are revealed the ability to carry vertical loads in compression and to accommodate shear deformations. The rubber layers, reinforced with steel shims, reduce the freedom to bulge by increasing the vertical stiffness of the bearing. Three types of laminated rubber bearings are widely used as seismic isolation devices: natural rubber bearing (RB), lead rubber bearing (LRB), and high damping rubber bearing (HDRB). RB occupies flexibility property and small damping and hence it has been used to accommodate the thermal movement, the effects of pre-stressing, creep, and shrinkage of superstructure of elevated highway or it has been used in seismic isolation by combining with other energy dissipation devices, such as lead, steel and viscous damper, etc. (Khan et al., 2015). Other two types of bearings possess high damping which are developed and widely used in various civil infrastructures including bridges in many countries, especially in Japan and USA (Khan, 2016). HDRB possess a variety of mechanical properties, which are influenced by their compounding effect, nonlinear elasto-plastic behaviour and temperature and strain-rate dependent viscosity property (Bhuiyan, 2009; Khan, 2016). Lead rubber bearings also acquire all the mechanical properties of

HDRB with reduced extent (Bhuiyan, 2009; Khan, 2016). LRB experiences some consequence-problems when subjected to strong earthquake excitations, especially the near field (NF) earthquake ground motions (Ozubulut and Hurlebaus, 2011a; 2011b). The unfortunate coincidence of the natural period of the seismically isolated bridge with that of the NF earthquakes amplifies the seismic responses of isolation system. In particular, LRB experiences large horizontal deformation under NF earthquakes which cause detrimental problems, such as instability of the bearings, pounding and unseating problems of the bridge deck (Choi, 2005; Khan, 2016). In recent years, a number of attempts are reported, by combining LRBs and shape memory alloy (SMA) in seismic isolation of highway bridges, to partially solve the above mentioned limitations (Khan et al., 2015). The super-elasticity accompanied by hysteresis property of the SMA allows it to fabricate with LRBs to reduce the residual deformation of the bridge system for sustainable seismic protection (Khan, 2016).

The objective of this work is to carry out seismic performance analysis of a bridge acted upon by far field (FF) earthquake ground accelerations in longitudinal direction. In this regard, nonlinear dynamic analysis of a bridge pier using a direct time integration approach is carried out. Two types of isolation bearings are employed in the analysis: lead rubber bearing (LRB) and smart material based laminated rubber bearing (SRB). The LRB (Fig.1a) is manufactured by alternating rubber layers with steel shims along with lead plugs to be inserted through bearing while the SRB (Fig.1b) comprises Ni-Ti and Cu-Be-Al based SMA wires with natural rubber bearing. In nonlinear dynamic analysis, the force-displacement behaviours of LRB and SRBs are evaluated using visco-elasto-plastic models. In addition, bilinear and linear elastic models are used for the bridge pier and deck, respectively. The variation of seismic responses of the bridge due to the use of LRB and SRBs are explored in the study. The bridge responses considered in this study include the peak values of pier displacement, bearing displacement, deck displacement, deck acceleration, bearing force and residual displacement. The comparison shows that the seismic responses of the bridge are affected by the use of two types of isolation bearings; more specifically, the residual displacements of the bridge pier are distinctly reduced in the case of SRBs in compare to LRB for all FF ground motions considered (Khan, 2016).

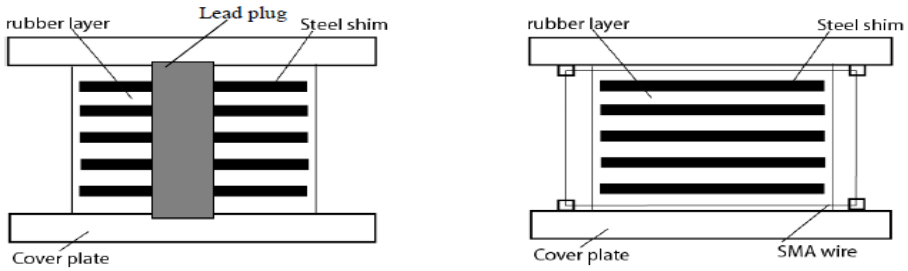

(a) (b)

Fig.1: Schematic details of (a) Lead Rubber Bearing (LRB) and (b) Shape Memory Alloy (SMA) based Rubber Bearing (SRB) (After Khan, 2016)

MODELING OF ELEVATED HIGHWAY

Physical Model of the Elevated Highway

A typical three-span continuous elevated highway, isolated by LRB and SRBs, is used in the current study. The bridge consists of continuous reinforced concrete (RC) deck-steel girder isolated by LRB and SRBs installed below the steel girder supported on RC piers. The superstructure consists of 260 mm RC slab covered by 80 mm of asphalt layer. The height of the continuous steel girder is 1800 mm. The mass of a single span elevated highway deck is 600×10^3 kg and that of a pier is 240×10^3 kg. The mass calculation procedure will be available in literature (Khan, 2016). The substructure consists of RC piers and footings supported on shallow foundation. The representative physical model as well as analytical model of the elevated highway is tried to given hereunder (Fig.2). The dimensions and material properties of the deck and piers of elevated highway with footings are given in Table 1.

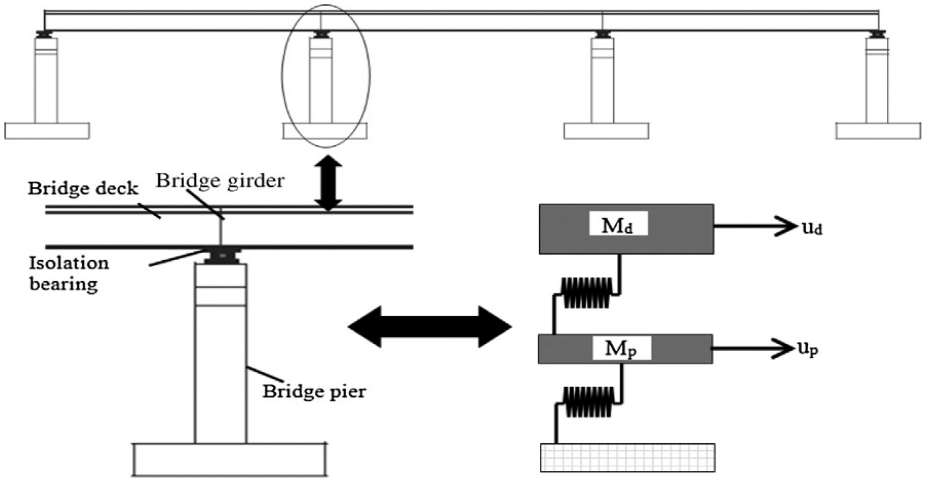

(a) (b)

Fig.2: Modelling of the elevated highway (a) physical model and (b) analytical model (After Khan, 2016)

Table 1: Geometries and material properties of the elevated highway (After Khan et al., 2015)

Properties	Specifications
Cross-section area of the pier cap (mm^2)	2000x12000
Cross-section area of the pier body (mm^2)	2000x9000
Height of the pier (mm)	15000
Young's modulus of elasticity of concrete (N/mm^2)	25000
Young's modulus of elasticity of steel (N/mm^2)	200000

ANALYTICAL MODEL OF THE ELEVATED HIGHWAY

Modelling of the Elevated Highway

The elevated highway model is simplified into a two-degree of freedom (2-DOF) system: one at the deck level and the other at the pier top level of the elevated highway. This simplification holds true only when the superstructure of elevated highway is assumed to be rigid in its own plane which shows no significant structural effects on the seismic performance of the elevated highway when subjected to earthquake ground acceleration in longitudinal direction. The mass proportional damping of the pier of elevated highway is considered in the analysis. Equations that govern the dynamic responses of the 2-DOF system can be derived by considering the equilibrium of all forces acting on it using the d'Alembert's principle. In this case, the internal forces are the inertia forces and the restoring forces, while the external forces are the earthquake induced forces. Equations of motion are given as,

$$m_p\ddot{u}_p(t)+F_p(u_p,t)-F_{is}(t)=-m_p\ddot{u}_g(t); \quad (1a)$$

$$m_d\ddot{u}_d(t)+F_{is}(t)=-m_d\ddot{u}_g(t); \quad (1b)$$

where, m_p, m_d, u_p and u_d are the masses and displacements of pier and deck, respectively. $\ddot{u}_p$ and $\ddot{u}_d$ are the accelerations of pier and deck, respectively. $\ddot{u}_g$ is the ground acceleration. F_p is the internal restoring force of the pier. F_{is} is the restoring force of the isolation bearings (LRB and SRB). The unconditionally stable Runge Kutta 4th order method is used in the direct time integration of the equations of motion (Eq. 1a and Eq. 1b) (Bhuiyan, 2009; Khan et al., 2015; Khan, 2016).

Modelling of the Pier of Elevated Highway

The pier is restricted to participate in energy absorption in the elevated highway in addition to the isolation bearing. The secondary plastic behaviour was expected to be lumped at bottom of the pier where plastic hinge is occurred. The plastic hinge of the pier is modeled by nonlinear spring element. Four hysteresis models for the nonlinear spring are usually used in the nonlinear dynamic analysis of an elevated highway: elasto-plastic model, bilinear model, Clough degradation model, and tri-linear Takeda model. In the current study, the nonlinear spring element is modeled using the bilinear model. The ratio of the post yield stiffness with elastic stiffness is considered as 0.01 (Khan, 2016).

Modelling of the LRB and SRB

The experimental investigations of LRB have revealed the four different fundamental properties, which together characterize the typical overall response: (i) a dominating elastic ground stress response, which is characterized by large elastic strains, (ii) a finite elasto-plastic response associated with relaxed equilibrium states, (iii) a finite strain-rate dependent viscosity induced overstress, which is portrayed by relaxation tests, and (iv) a damage response within the first cycles, which induces considerable stress softening in the subsequent cycles. Considering the first three properties, a strain-rate dependent constitutive model for the LRB was developed by Bhuiyan (2009) which is verified for sinusoidal excitations and subsequently implemented in seismic analysis using professional software (Resp-T, 2006). The geometries and material properties of LRB are presented by Table 2.

Table 2: Geometries and materials properties of the laminated rubber bearing (After Khan, 2016)

Sl. No.	Particulars	Value
01	Cross section of the bearing (mm^2)	1000000
02	Thickness of the rubber layers (mm)	200
03	Number of rubber layers	6
04	Thickness of steel layer (mm)	3.0
05	Nominal shear modulus of rubber (MPa)	1.2

The constitutive model of SMAs is very complicated in a sense that it depends upon many factors, such as strain rates, strain magnitude and strain history. Three categories of constitutive models are used for characterizing the super-elasticity and damping properties of SMA bar, such as parametric, nonparametric and differential equation-based models (Khan et al., 2015). However, the differential equation-based constitutive model is widely used for SMAs since it is capable of using in continuum mechanics based finite element algorithms considering small and finite deformations and subsequently in finite element based professional software packages. In realization, the complexity of replicating the mechanical behaviour of SMAs by the use of phenomenological models, three versions of the models are used in seismic applications. The models include a simplified model, which is constructed based on experimentally obtained data; a thermo-mechanical model, which considers the stress-strain-temperature relationship in SMAs; and a thermo-mechanical model, which also takes into account the cyclic loading effects in SMAs. In recognizing the intricacy of the phenomenological models considering the thermo-mechanical behaviour of SMAs, a simplified model (Bhuiyan and Alam, 2013) is used to model the SRBs. Table 3 shows the geometries and material properties of the Copper-Beryllium-Aluminium (Cu-Be-Al) and Nitinol (Ni-Ti) SMA wires used in this study.

Table 3: Geometries and materials properties of SMA wires used in the analysis (After Khan, 2016)

Sl. No.	Particulars	SMA bar (Cu-Be-Al)	SMA bar (Ni-Ti)
01	Modulus of Elasticity (N/mm^2)	32040	72000
02	Yield Strength (N/mm^2)	235	270
03	Length of Wires (mm)	2500	2500
04	Cross Sectional Area (mm^2)	600	600

SEISMIC GROUND ACCELERATION

By Caltrans (2004), if the structure under consideration is within 10 miles (approx. 15 km) of a seismic fault can be classified as NF. Ground motions outside this range are classified as FF motions. Current study considers a suite of five FF ground motion records of medium to strong earthquakes with peak ground acceleration (PGA) values ranging from 0.243g to 0.728g (Fig.3(a) to 3(e)). Fig.3(f) shows the characteristics of the ground motions performing response spectrum analysis with 5 percent damping ratio. Here, the dominant periods of the ground motion records delimited by 0.2 to less than 1.0 sec which cover the wide range of natural period of bridge structures (Khan, 2016).

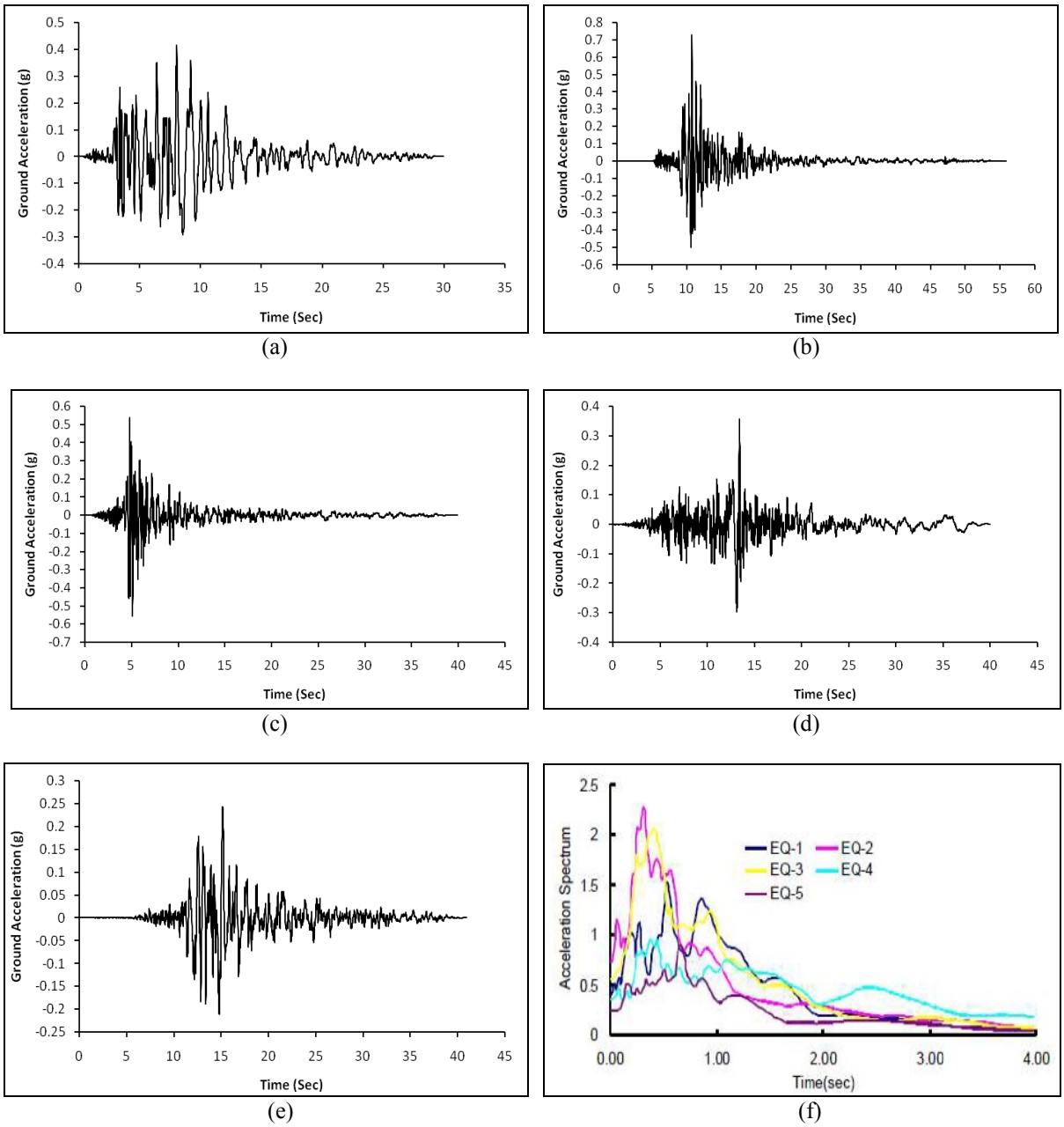

Fig.3 Acceleration time histories of far field seismic ground motion records; (a) EQ-1, (b) EQ-2, (c) EQ-3, (d) EQ-4, (e) EQ-5 and (f) Acceleration response spectra

NUMERICAL RESULTS AND DISCUSSION

In comparative assessment, a few standard response parameters obtained for each earthquake ground motion are addressed in the subsequent subsections: pier displacement, bearing displacement, deck acceleration, deck displacement, residual displacement of the deck of elevated highway after earthquake and bearing force (Bhuiyan and Alam, 2013). Each response parameter of the system

equipped with LRB is compared with SRBs. For convenience, Ni-Ti SMA based laminated rubber bearing is expressed by "SRB 1" and Cu-Be-Al SMA based laminated rubber bearing is expressed by "SRB 2". The numerical outcomes of a single representative earthquake (EQ-2) were placed in this article due to page limitation. Numerical outcomes for rest of the seismic records are available in literature (Khan, 2016). Fig.4 to Fig.10 presents typical responses of the elevated highway for EQ-2. The trends of the results obtained from absolute maximum responses by nonlinear dynamic analysis are exhibits through Fig.11 to Fig.13. The simulation results are summarized in Table 4 for both the LRB and SRBs when considering far field ground motion record EQ-1 to EQ-5 respectively.

Pier Displacement

The pier displacement decreases with increase in energy dissipation but increases with increase in the bearing forces. Therefore, the SRBs usually produce larger pier displacement than LRB. Fig.4 to Fig.6 exhibits time histories of the pier displacement due to EQ-2 when considering LRB, SRB 1 and SRB 2, respectively. Fig.11 confirmed that, the LRB and SRB 2 possess maximum (48.145mm) and minimum (38.180 mm) pier displacements whereas SRB 1 possess in the middle (41.301 mm) for seismic ground motion EQ-1. Again, Fig.11 argued that, the SRB 1 and LRB possess maximum (81.334 mm) and minimum (57.874 mm) pier displacements whereas SRB 2 possess in the middle (80.546 mm) for seismic ground motion EQ-2. Similarly, Fig.11 established that, the LRB and SRB 1 possess maximum (32.688 mm) and minimum (26.203 mm) pier displacements whereas SRB 2 possess in the middle (30.333 mm) for seismic ground motion EQ-3. Furthermore, Fig.11 says that, the SRB 1 and LRB possess maximum (47.943 mm) and minimum (36.150 mm) pier displacements whereas SRB 2 possess in the middle (44.721 mm) for seismic ground motion EQ-4. Moreover, Fig. 4.36 revealed that, the LRB and SRB 2 possess maximum (37.774 mm) and minimum (33.564 mm) pier displacements whereas SRB 1 possess in the middle (37.717 mm) for ground motion EQ-5.

Bearing Displacement

The bearing displacements are obtained from relative displacements between deck and pier. Bearing displacement increases with the decrease in energy dissipation of the bearings as revealed from Fig.10. It appears from the Figs.7 to Fig.9 that, the residual displacements of SRBs are bigger in magnitude than LRB, which correspond to the observations of the pier displacements. Fig.7 to Fig.9 exhibits time histories of the bearing displacement due to EQ-2 when considering LRB, SRB 1 and SRB 2, respectively. Fig.12 confirmed that, the SRB 1 and LRB possess maximum (202.703 mm) and minimum (185.765 mm) bearing displacements whereas SRB 2 possess in the middle (200.621 mm) for ground motion EQ-1. Again, Fig.12 argued that, the SRB 2 and LRB possess maximum (241.884 mm) and minimum (193.969 mm) bearing displacements whereas SRB 1 possess in the middle (195.929 mm) for ground motion EQ-2. Again, Fig.12 established that, the LRB and SRB 1 possess maximum (71.969 mm) and minimum (62.099 mm) bearing displacements whereas SRB 2 possess in the middle (65.508 mm) for ground excitation EQ-3. Furthermore, Fig.12 says that, the SRB 2 and LRB possess maximum (157.302 mm) and minimum (140.609 mm) bearing displacements whereas SRB 1 possess in the middle (155.262 mm) for ground motion EQ-4. Moreover, Fig. 4.37 revealed that, the LRB and SRB 2 possess maximum (130.473 mm) and minimum (117.673 mm) bearing displacements whereas SRB 1 possess in the middle (119.893 mm) for ground excitation EQ-5.

Residual Displacement

The residual displacement of the bearing is computed by taking the arithmetic average of the stable absolute values of the last 5 to 15 sec of the time history of bearing displacements as obtained from the dynamic analysis of the system for each earthquake (Khan, 2016). The residual displacements of SRBs are smaller than LRB for all earthquakes as presented in tenth column of Table 4. For seismic ground motion record EQ-1, Fig.13 confirmed that, the LRB and SRB 2 possess maximum (7.796 mm) and minimum (2.980 mm) residual displacements whereas SRB 1 possess in the middle (3.165 mm). Again, for seismic ground motion record EQ-2, Fig.13 argued that, the LRB and SRB 1 possess maximum (7.928 mm) and minimum (3.141 mm) residual displacements whereas SRB 2 possess in the middle (3.456 mm). Similarly, for seismic ground motion record EQ-3, Fig.13 established that, the LRB and SRB 2 possess maximum (8.114 mm) and minimum (3.031 mm) residual displacements

whereas SRB 1 possess in the middle (3.203 mm). Furthermore, for seismic ground motion record EQ-4, Fig.13 says that, the LRB and SRB 2 possess maximum (10.135 mm) and minimum (3.673 mm) residual displacements whereas SRB 1 possess in the middle (3.737 mm). Moreover, for ground motion record EQ-5, Fig.13 revealed that, the LRB and SRB 2 possess maximum (7.696 mm) and minimum (2.881 mm) residual displacements whereas SRB 1 possess in the middle (3.178 mm).

Table 4: Absolute maximum seismic responses of LRB, SRB 1 & SRB 2 due to Earthquake EQ-1 to EQ-5

EQ	Time (Sec)	PGA (g)	Bearing Type	Bearing Disp. (mm)	Deck Acc. (m/sq.s)	Pier Disp. (mm)	Deck Disp. (mm)	Bearing Force (kN)	Residual Disp. (mm)
EQ-1	30	0.416	LRB	185.765	4.337	48.145	172.321	1241.323	7.796
EQ-1	30	0.416	SRB 1	202.703	5.143	41.301	211.943	1616.841	3.165
EQ-1	30	0.416	SRB 2	200.621	4.557	38.180	202.573	1394.977	2.980
EQ-2	60	0.728	LRB	193.969	6.174	57.874	218.873	1219.012	7.928
EQ-2	60	0.728	SRB 1	195.929	5.726	81.334	201.989	1587.320	3.141
EQ-2	60	0.728	SRB 2	241.884	5.962	80.546	247.160	1608.637	3.456
EQ-3	40	0.555	LRB	71.969	5.521	32.688	65.431	793.803	8.114
EQ-3	40	0.555	SRB 1	62.099	5.491	26.203	63.276	815.710	3.203
EQ-3	40	0.555	SRB 2	65.508	5.490	30.333	63.054	764.116	3.031
EQ-4	40	0.358	LRB	140.609	3.590	36.150	138.975	1006.031	10.135
EQ-4	40	0.358	SRB 1	155.262	3.632	47.943	171.956	1351.781	3.737
EQ-4	40	0.358	SRB 2	157.302	3.691	44.721	166.166	1182.712	3.673
EQ-5	40	0.243	LRB	130.473	2.837	37.774	126.366	998.194	7.696
EQ-5	40	0.243	SRB 1	119.893	2.893	37.717	122.745	1139.470	3.178
EQ-5	40	0.243	SRB 2	117.673	2.868	33.564	117.655	995.744	2.881

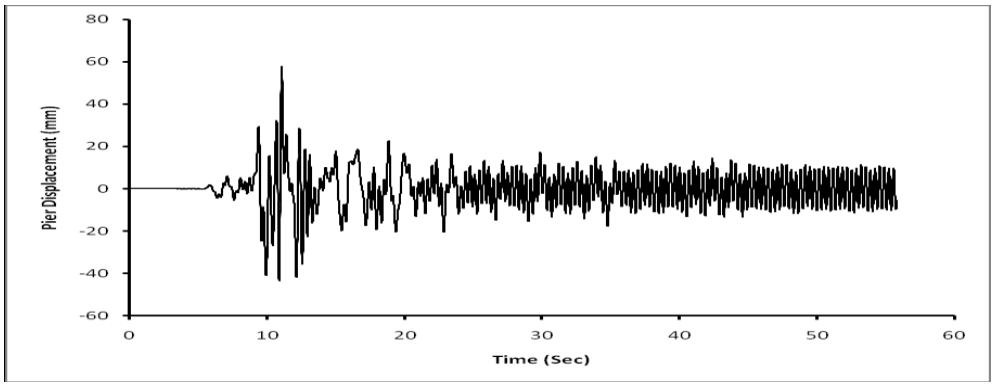

Fig.4: Pier displacement due to EQ-2 when considering LRB

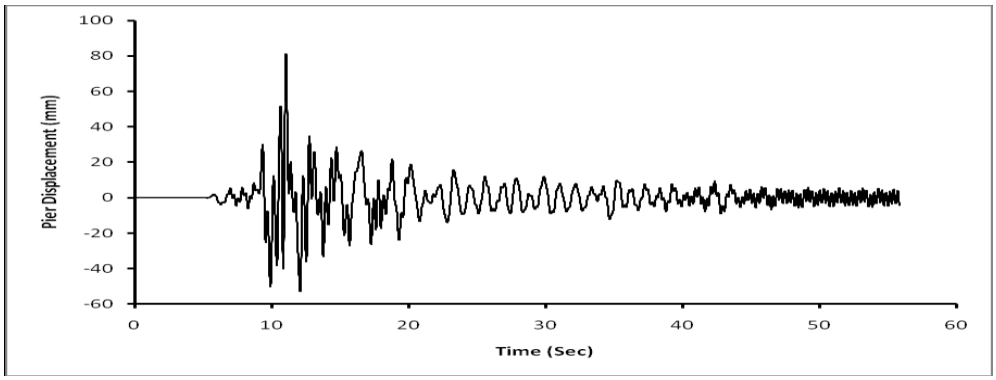

Fig.5: Pier displacement due to EQ-2 when considering SRB 1

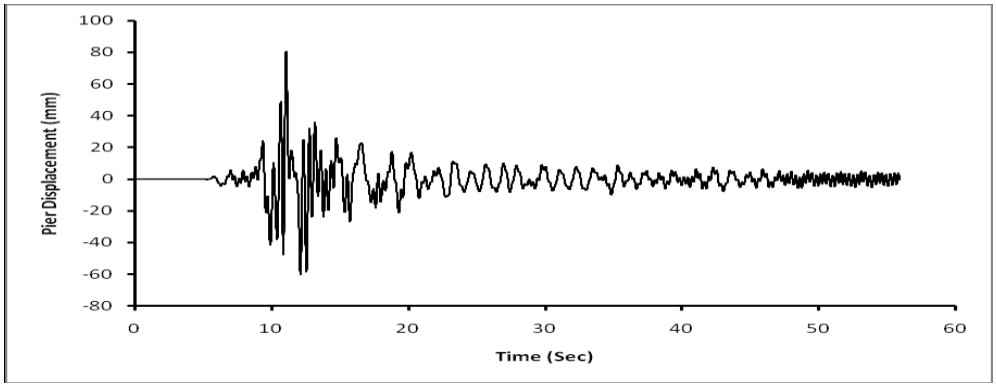

Fig.6: Pier displacement due to EQ-2 when considering SRB 2

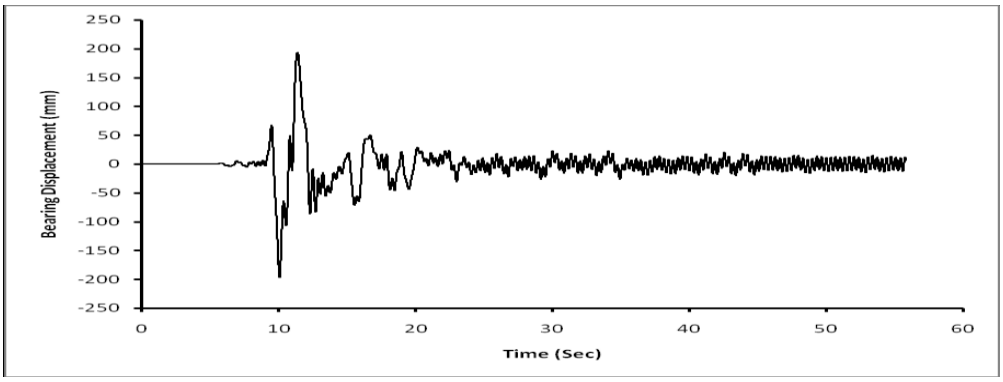

Fig.7: Bearing displacement due to EQ-2 when considering LRB

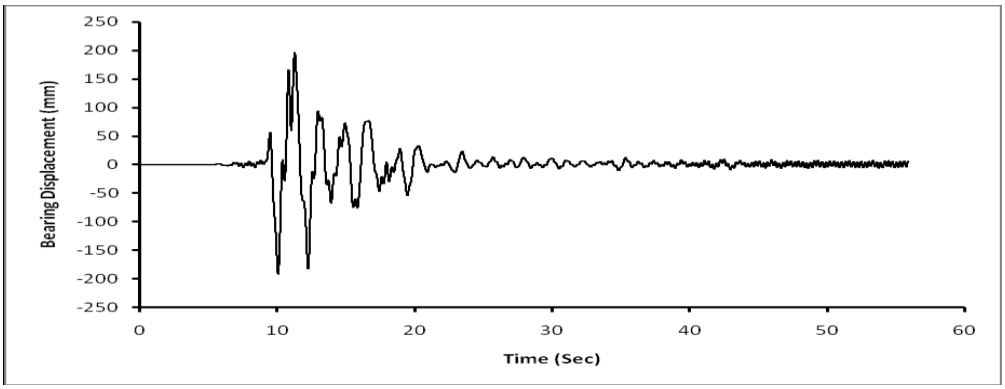

Fig.8: Bearing displacement due to EQ-2 when considering SRB 1

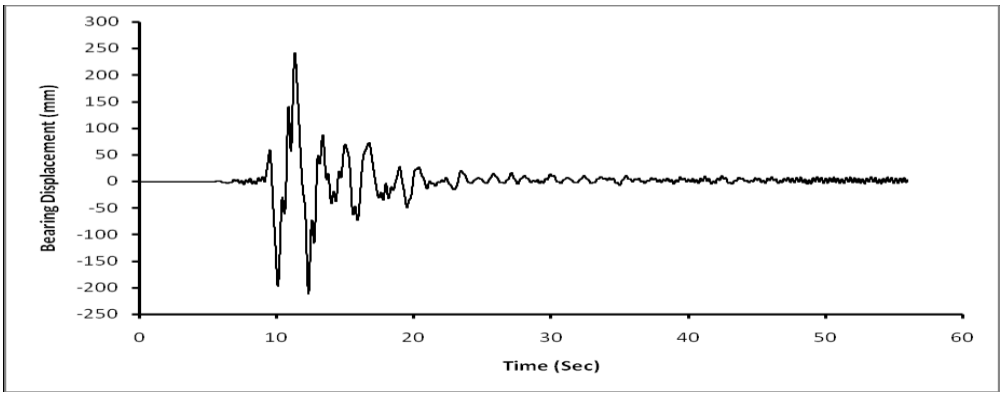

Fig.9: Bearing displacement due to EQ-2 when considering SRB 2

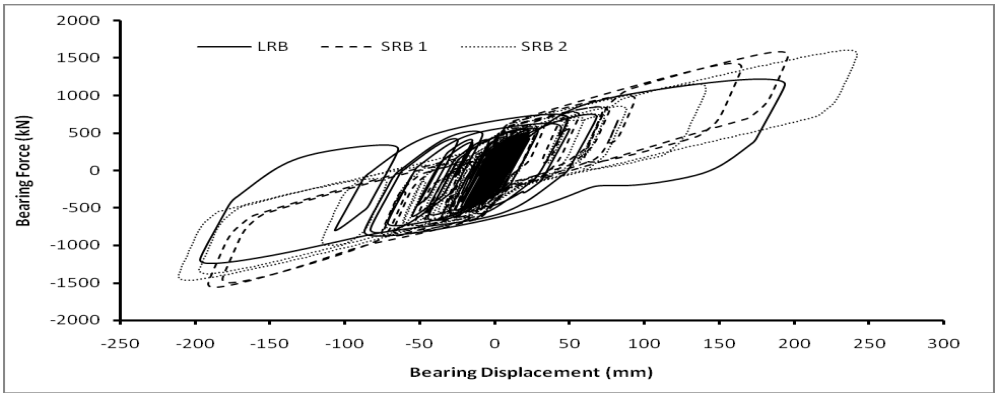

Fig.10: Comparison of force-displacement relationship for LRB, SRB 1 and SRB 2 due to EQ-2

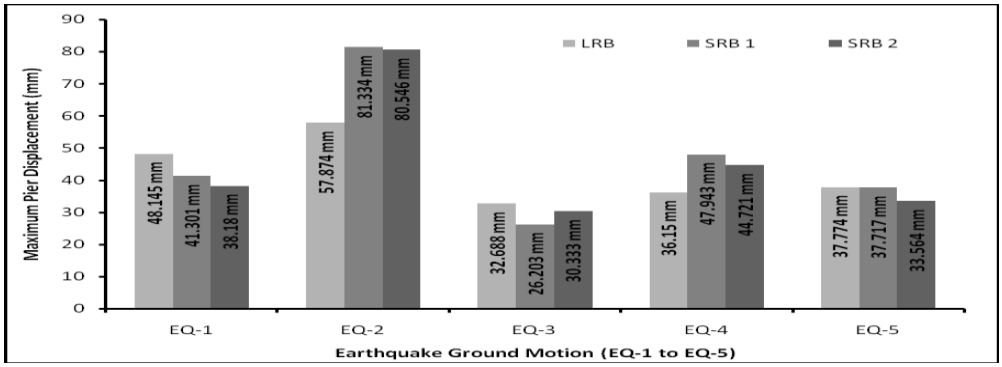

Fig.11: Comparison of maximum pier displacement for LRB, SRB 1 and SRB 2 due to EQ-1 to EQ-5

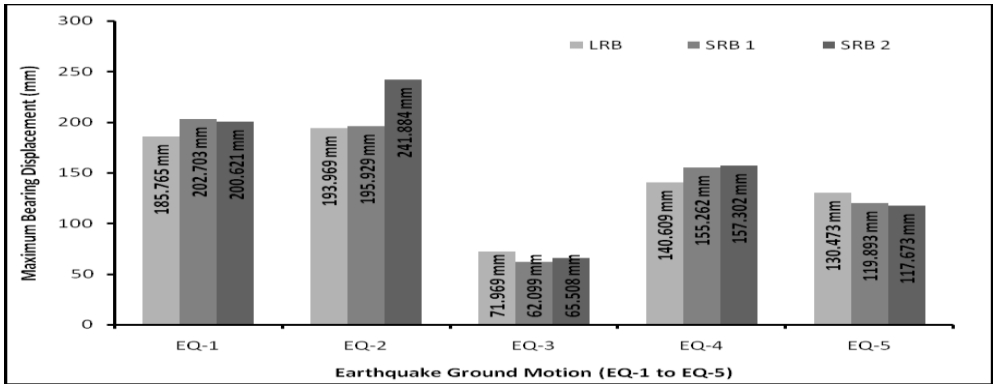

Fig.12: Comparison of maximum bearing displacement for LRB, SRB 1 and SRB 2 due to EQ-1 to EQ-5

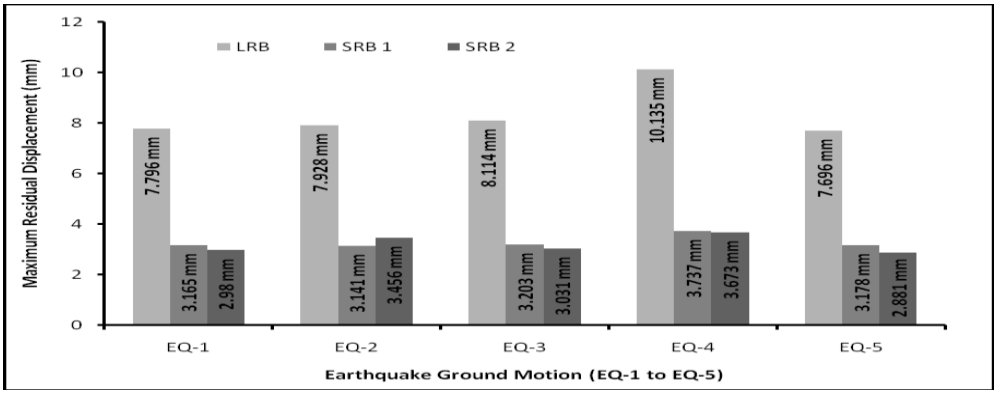

Fig.13: Comparison of maximum residual displacement for LRB, SRB 1 and SRB 2 due to EQ-1 to EQ-5

CONCLUDING REMARKS

This study presents the seismic performance assessment of an elevated highway isolated by lead rubber bearing (LRB) and SMA based natural rubber bearing (SRB). Two types of SRB have been employed in this analysis to initiate the seismic performance assessment of elevated highway by nonlinear dynamic analysis. These are Ni-Ti based laminated rubber bearing (SRB 1) and Cu-Be-Al based laminated rubber bearing (SRB 2). The nonlinearity of the bridge pier was considered by employing a bilinear force-displacement relationship developed by Bhuiyan (2009). A fixed restraint condition at bottom of the pier was considered. A complicated strain-rate dependent constitutive model for the LRB was used where as a visco-elasticity based analytical model was utilized for SRBs (Bhuiyan and Alam, 2013). The seismic performance considered in this studies are pier displacement, deck displacement, bearing displacement, deck acceleration, bearing force and residual displacement (Khan et al., 2015). The numerical results have revealed that, the SRBs satisfactorily restrain the residual displacement of the deck and the displacement of the pier of elevated highway for a suite of five FF ground motion records considered in this study. However, for deck and bearing displacements, the elevated highway with LRB has usually resulted in smaller responses in compared to SRBs. Almost a similar trend was observed in the case of deck accelerations. The early activation of hardening effect of SRBs in compared to LRB might have significant effect on the seismic responses of the system. The LRB designed in this study shows a larger dissipation of energy than that of SRBs. From the numerical analysis, it appears that not only the magnitude but the other characteristics of earthquake ground motions also have significant effect on the seismic responses of the elevated highway which should be carefully considered at design phase.

REFERENCES

Bhuiyan, AR. 2009. *Rheology modeling of laminated rubber bearings,* PhD dissertation, Graduate School of Science and Engineering, Saitama University, Japan.

Bhuiyan, AR and Alam, MS. 2013. Seismic performance assessment of highway bridges equipped with superelastic shape memory alloy-based laminated rubber isolation bearing, *Engineering Structures,* 49:396–407.

California Dept. of Transportation (CALTRANS), 2004. *Seismic Design Criteria,* Sacramento, USA.

Choi, E; Nam, T and Cho, B. 2005. A new concept of isolation bearings for highway steel bridges using shape memory alloys, *Canadian Journal of Civil Engineers,* 32:957–967.

Khan AKM TA; Bhuiyan, MAR and Alam, MS. 2015. Use of Ni-Ti shape memory alloy bars in seismic retrofit of multi-span elevated highway*, Proceedings of the National Conference of Earthquake and Environmental Disaster (NCEED - 2015*), CUET, Chittagong, Bangladesh.

Khan, AKM, TA. 2016. *Use of Shape Memory Alloy in Seismic Retrofit of Multi-Span Simply Supported Elevated Highway,* PGD Project Report, IEER, CUET, Chittagong, Bangladesh.

Ozbulut, OE and Hurlebaus, S. 2011a. Optimal design of superelastic-friction base isolators for seismic protection of highway bridges against near-field earthquakes, *Earthquake Engineering & Structural Dynamics,* 40: 273–291.

Ozbulut, OE and Hurlebaus, S. 2011b. Seismic assessment of bridge structures isolated by a shape memory alloy or rubber-based isolation system, *Smart Materials and Structures,* IOP Publishing Ltd, 20: 1-12.

Resp-T, 2006. *User's Manual for Windows,* Version 5.